AIAA JOURNAL
Vol. 34, No. 4, April 1996

Mode Shape Expansion Techniques for Prediction: Experimental Evaluation

Marie Levine-West,* Mark Milman,† and Andy Kissil‡
Jet Propulsion Laboratory, California Institute of Technology, Pasadena, California 91109-8099

Mode shape expansion techniques fall under four broad categories. Spatial interpolation methods use geometric information to infer mode shapes at unmeasured locations. Direct methods use the dynamic equations of motion to obtain closed-form solutions to the expanded eigenvectors. These methods can be interpreted as constrained optimization problems. Projection methods use a least-squares formulation that also can be formulated through constrained optimization. Error methods use a formulation that can account for uncertainties in the measurements and in the prediction. This includes penalty methods and the new expansion techniques based on least-squares minimization techniques with quadratic inequality constraints (LSQI). Some of these expansion techniques are selected herein for evaluation using the full set of experimental data obtained on the microprecision interferometer test bed. Both a pretest and an updated analytical model are considered in the trade study. The robustness of these methods is verified with respect to measurement noise, model deficiency, number of measured degrees of freedom, and accelerometer location. It is shown that the proposed LSQI method has the best performance and can reliably predict mode shapes, even in very adverse situations.

Nomenclature

a	= measured degrees-of-freedom (DOF) aset
K	= $(N \times N)$ full stiffness matrix
M	= $(N \times N)$ full mass matrix
N	= full set of DOF, $a + o$
o	= nonmeasured DOF, $o$set
P_{pp}	= $(p \times p)$ orthogonal Procrustes transformation matrix
p	= number of modes
θ_{si}	= strain energy for mode i in element s
$\Phi_{Np}, \tilde{\Phi}_{Np}, \hat{\Phi}_{Np}$	= $(N \times 1)$ matrix of p analytical/test/expanded eigenvectors at full set of DOF
$\phi_{ai}, \tilde{\phi}_{ai}, \hat{\phi}_{ai}$	= $(a \times 1)$ ith analytical/test/expanded eigenvector at measured DOF
$\phi_{oi}, \tilde{\phi}_{oi}, \hat{\phi}_{oi}$	= $(o \times 1)$ ith analytical/test/expanded eigenvector at nonmeasured DOF
$\omega_i, \tilde{\omega}_i$	= ith analytical/test modal frequencies
$\sim$	= actual test data
$\hat{}$	= expanded test data

I. Introduction

IN the companion paper,[1] several mode shape expansion methods are introduced. Mode shape expansion has applications for mode shape visualization, for test-analysis correlation at all the degrees of freedom (DOFs) of finite element method (FEM) structural models, and for response prediction at unmeasured DOFs in structural integrity assessments to dynamic loads. Control needs for mode shape expansion include computation of the strain energy distributions for optimal damper and active member placement in vibration attenuation problems, and tuning of multi-input/multi-output control parameters and gains.

This study evaluates the robustness and reliability of several mode shape expansion methods presented in the companion paper.[1] The methods used for comparison of mathematical and structural performance metrics are 1) the Guyan static expansion method, 2) the Kidder dynamic method, 3) the Procrustes method, and 4) the new penalty method and least-squares minimization techniques with quadratic inequality constraints (LSQI method). Spatial interpolation methods will not be included in this study because they are not suitable for most structures. Sensitivity studies are performed using actual experimental data obtained on the Jet Propulsion Laboratory (JPL) micro-precision interferometer (MPI) truss. Two independent modal tests were performed on the MPI, one of which measured the response at 240 DOFs along the structure.[2] The first 15 modes up to 60 Hz were identified. A 10,000-DOF model was then derived that correlated with all 15 modes up to 60 Hz.[3]

The study involves taking a subset of the actual set of instrumented DOFs, and verifying the accuracy of the expanded prediction. The methods are evaluated as to their sensitivity to combinations of measurement error and distributed and localized modeling errors. Sensitivity to modeling error is evaluated by using both the approximate pretest FEM model and reconciled updated model. The performance of the modal expansion techniques is also assessed with respect to sensor quantity and location. It is shown that the new method derived from a least-squares minimization formulation with quadratic inequality constraint provides by far the most reliable mode shape estimates, even in adverse situations.

II. MPI Test Bed

MPI test bed at the JPL is a 210-kg lightly damped truss structure composed of two booms and a vertical tower 7 × 6.3 × 5.5 m. The MPI finite element model geometry is shown in Fig. 1. The

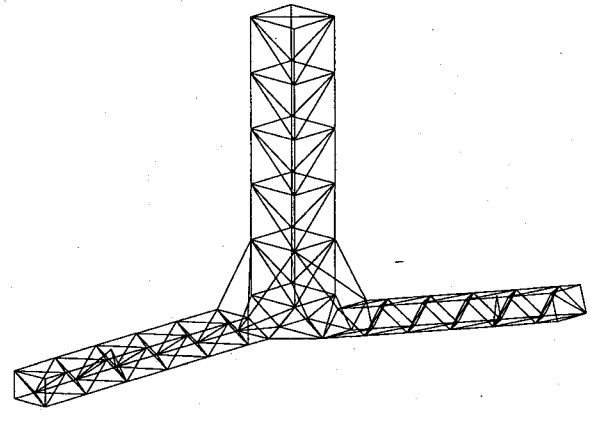

Fig. 1 Finite element model of the MPI test bed.

Received Dec. 15, 1994; revision received April 26, 1995; accepted for publication Oct. 10, 1995. Copyright © 1996 by the American Institute of Aeronautics and Astronautics, Inc. The U.S. Government has a royalty-free license to exercise all rights under the copyright claimed herein for Governmental purposes. All other rights are reserved by the copyright owner.

*Technical Group Leader, Science and Technology Development Section, 4800 Oak Grove Drive, M.S. 157-316.
†Member, Technical Staff, Automation and Control Section.
‡Member, Technical Staff, Mechanical Engineering Section.

Table 1 MPI modal test results: frequency error, mode shape error [Eq. (10)], and test MAC [Eq. (13)]

Mode no.	Freq., Hz	ΔF, %	$\Delta\phi$, %	Test MAC
1	7.75	0.46	10.24	0.99
2	11.65	0.11	11.89	0.99
3	12.67	0.66	7.43	0.99
4	29.36	0.59	19.32	0.96
5	34.06	0.60	24.36	0.94
6	37.34	0.56	12.30	0.98
7	42.25	0.88	8.07	0.99
8	46.04	0.18	11.34	0.99
9	49.50	0.14	16.51	0.97

MPI is composed of 250 aluminum struts connected to 80 node balls. The careful design of the strut-to-node assembly ensures linearity in the response.[2] The primary objective of the MPI is to perform system integration of control-structure interaction technologies to demonstrate the end-to-end operation of a space-based optical interferometer.[4] The high imaging resolution of future space missions will require a 15-nm rms control of the optical pathlength over the 7-m baseline of the structure. Accurate modeling and response prediction are essential for the successful implementation of these control objectives.

Detailed modal testing was performed on the MPI, and modal parameter identification was achieved for the first 15 structural modes up to 60 Hz.[2] For the purpose of this analysis, only the first nine structural modes up to 50 Hz are considered. The accuracy of the experimental procedures is substantiated by two independent sets of modal tests, carried out with distinct equipment, processors and personnel. The two modal tests measured 240 and 164 DOFs of the structure, respectively. As shown in Table 1, the accuracy of the identified modal frequencies, ΔF, is of the order of 0.5% and the modal assurance criteria (MAC) [Eq. (13)] between the two sets of mode shapes is greater than 0.98 for most of the modes. However, the accuracy of the identified mode shapes at the common 164 DOFs, $\Delta\phi$ [Eq. (10)], is only of the order of 15%. This infers that mode shape values are highly uncertain, even with precise test procedures, excellent frequency repeatability, and better-than-average MAC. In Sec. IV, it also is demonstrated that the MAC are not sensitive metrics for mode shape error since they are related to the angle cosines between two vectors, such that for small errors MAC $\approx 1-(\Delta\phi)$ (Refs. 2 and 5).

A pretest FEM model of the MPI structure was designed with 250 axial rod elements (1 per strut) and 240 DOFs (3 DOFs at each of the 80 node balls). In Table 2, the modal properties predicted by the pretest FEM model are compared to the experimental frequencies and mode shapes. The pretest model has modal frequency errors of the order of 5%, and mode shape errors of the order of 25%, with the largest errors in the higher modes. Again, the MAC are not sensitive performance metrics, since mode shape errors of 40% correspond to MAC of 0.84. Table 2 also demonstrates that the mass cross-orthogonality [MX, Eq. (16)] is even less sensitive than the MAC since it is biased toward the DOFs with larger mass and kinetic energy participation: mode shape errors of 40% correspond to an MX of 92%.

The model was later improved by a combination of subcomponent testing and full model Bayesian estimation.[3] A final FEM model was derived with approximately 1500 beam elements and 10,000 DOFs. The updated model correlates extremely well to the test data since it has errors of less than 1% in the frequencies and MAC of about 0.99 for the modes up to 50 Hz. For the purpose of this study, Guyan reduction was then performed, reducing the 10,000-DOF model to the same 240 DOFs measured during the modal test. As shown in Table 3, Guyan reduction has little effect on the accuracy of the analytical modes up to 50 Hz since the modal frequency errors with respect to the test data are still approximately 1%, the MAC are still of the order of 0.99, and the difference between the analytical and the experimental mode shapes, $\Delta\phi$, is less than the differences measured during the two independent sets of tests (Table 1). Only the two highest modes beyond 45 Hz have been slightly affected by the reduction process, but their estimates are still within the accuracy expected from the experimental procedure.

Table 2 MPI pretest model: frequency error, mode shape error [Eq. (10)], MAC [Eq. (13)] and MX [Eq. (16)] with respect to test data

Mode no.	Freq., Hz	ΔF, %	$\Delta\phi$, %	Model MAC	Test MX
1	7.67	1.00	5.64	1.00	1.00
2	11.43	1.90	7.12	0.99	1.00
3	12.47	1.54	6.33	1.00	1.00
4	27.38	6.73	8.54	0.99	1.00
5	32.80	3.68	31.26	0.90	0.95
6	34.23	8.33	36.94	0.86	0.93
7	38.52	8.83	24.47	0.94	0.97
8	44.59	3.14	30.19	0.91	0.95
9	46.99	5.07	39.38	0.84	0.92

Table 3 MPI updated model: frequency errors, mode shape error [Eq. (10)], MAC [Eq. (13)] and MX [Eq. (16)] with respect to test data

Mode no.	Freq., Hz	ΔF, %	$\Delta\phi$, %	Model MAC	Test MX
1	7.82	0.88	5.70	1.00	1.00
2	11.66	0.11	8.26	0.99	1.00
3	12.75	0.67	7.42	0.99	1.00
4	29.52	0.56	6.71	1.00	1.00
5	34.45	1.16	6.04	1.00	1.00
6	37.76	1.12	9.82	0.99	0.99
7	42.81	1.32	9.61	0.99	1.00
8	47.30	2.74	15.18	0.98	0.99
9	51.14	3.30	26.88	0.93	0.96

The pretest FEM model and the exact updated FEM model are used in Sec. V to evaluate the sensitivity of the mode shape expansion techniques. Based on the results of the two independent modal tests, differences between the expanded and the measured mode shapes of less than 10% are considered valid.

III. Mode Shape Expansion Methods

A previous analysis has demonstrated that existing mode shape expansion techniques fall into four broad categories, each of which can be expressed in terms of a constrained optimization problem.[1] These methods are summarized as follows.

Direct methods use the dynamic equations of motions to obtain a closed-form solution of the expanded mode shape. This includes the Guyan (static) expansion method[5] and the Kidder (dynamic) expansion method.[6] The Guyan method can be interpreted as finding the expanded mode shape $\hat{\phi}_{Ni}$, which minimizes the total strain energy of mode i such that the predicted mode shape equals the test values at the measured DOFs a:

$$\min_{\hat{\phi}_{Ni}} \tfrac{1}{2}\langle \hat{\phi}_{Ni}, K\hat{\phi}_{Ni}\rangle, \qquad \text{subject to} \qquad \hat{\phi}_{ai} = \tilde{\phi}_{ai} \tag{1}$$

Similarly, the Kidder method finds the optimal expanded mode shape $\hat{\phi}_{Ni}$, which finds the stationary value of the residual dynamic energy of mode i such that the predicted mode shape equals the test values at the measured DOFs a:

$$\min_{\hat{\phi}_{Ni}} \langle \hat{\phi}_{Ni}, (K - \tilde{\omega}_i M)\hat{\phi}_{Ni}\rangle, \qquad \text{subject to} \qquad \hat{\phi}_{ai} = \tilde{\phi}_{ai} \tag{2}$$

The closed-form solutions to Eqs. (1) and (2) have been derived in the companion paper.[1]

Projection methods are formulated as a constrained quadratic optimization problem to minimize the error between a set of measured and expanded mode shapes. The Procrustes method,[7] which falls under this category, finds the orthogonal Procrustes transformation P_{pp} of the p experimental eigenvectors into the space spanned by the p predicted analytical eigenvectors at the measured DOF a:

$$\min_{P_{pp}} \left|\tilde{\Phi}_{ap} - \Phi_{ap}P_{pp}\right|_F^2, \qquad \text{subject to} \qquad P_{pp}^{\mathrm{T}}P_{pp} = I \tag{3}$$

where $|\cdot|_F$ denotes the Frobenius norm of a matrix,

$$|X|_F^2 = tr(X^{\mathrm{T}}X) \tag{4}$$

tr is the trace operator. The orthogonality constraint has the geometric interpretation of finding the best fitting rotation of analytical to experimental data. The mode is then extrapolated to the unmeasured DOF by this same rotation.

Error methods formulate the expanded mode shape in terms of the uncertainty in the measurement or in the model. Two error formulations have been proposed.[1] In the first approach, penalty methods are applied to Guyan expansion to minimize a weighted sum of the modal strain energy and the error in the measured mode shape.

PEN1:

$$\min_{\hat{\phi}_{Ni}} \tfrac{1}{2}\langle \hat{\phi}_{Ni}, K\hat{\phi}_{Ni}\rangle + \tfrac{1}{2}\gamma|\tilde{\phi}_{ai} - \hat{\phi}_{ai}|^2 \tag{5}$$

The analogous penalty method formulation is extended to include expansion error

PEN2:

$$\min_{\hat{\phi}_{Ni}} \tfrac{1}{2}\langle \hat{\phi}_{Ni}, K\hat{\phi}_{Ni}\rangle + \tfrac{1}{2}\gamma|\hat{\phi}^d_{ai} - \hat{\phi}_{ai}|^2 \tag{6}$$

where $\hat{\phi}^d_{Ni}$ is the mode shape obtained from a direct expansion method such as Eq. (2). Selection of the weighting parameter γ is discussed in the companion paper,[1] where it also is shown that as $\gamma \to \infty$, PEN1 and PEN2 converge to the Guyan and the Kidder solutions, respectively.

LSQI methods also have been proposed as a means to incorporate measurement uncertainty.[1] The hard constraints imposed by the direct methods have been relaxed to allow the solution to converge within the bound α expected from the experimental accuracy

LSQI1:

$$\min_{\hat{\phi}_{Ni}}\langle \hat{\phi}_{Ni}, K\hat{\phi}_{Ni}\rangle, \qquad \text{subject to} \qquad |\tilde{\phi}_{ai} - \hat{\phi}_{ai}|^2 \le \alpha|\tilde{\phi}_{ai}|^2 \tag{7}$$

As $\alpha \to 0$, LSQI1 converges to the Guyan static expansion in Eq. (1).

A second LSQI formulation also proposes to minimize the modal strain energy but subject to the constraint that the quadratic error between the optimally expanded mode shape $\hat{\phi}_{Ni}$, and the mode shape obtained from direct expansion $\hat{\phi}^d_{Ni}$ is less than the expected experimental error

LSQI2:

$$\min_{\hat{\phi}_{Ni}}\langle \hat{\phi}_{Ni}, K\hat{\phi}_{Ni}\rangle, \qquad \text{subject to} \qquad \left|\hat{\phi}_{Ni} - \hat{\phi}^d_{Ni}\right|^2 \le \alpha|\tilde{\phi}_{ai}|^2 \tag{8}$$

As $\alpha \to 0$, LSQI2 converges to the direct expansion solution $\hat{\phi}^d_{Ni}$ [Eq. (2)].

In yet a third formulation, the objective function is defined as the quadratic norm of the modal residual force such that the quadratic error between the expanded mode shape and the experimental mode shape at the measured DOFs is within the bounds expected from experimental error

LSQI3:

$$\min_{\hat{\phi}_{Ni}} |(K - \tilde{\omega}_i M)\hat{\phi}_{Ni}|^2, \qquad \text{subject to} \qquad |\hat{\phi}_{ai} - \tilde{\phi}_{ai}|^2 \le \alpha|\tilde{\phi}_{ai}|^2 \tag{9}$$

As $\alpha \to 0$, LSQI3 indirectly solves the eigenvalue problem for the given experimental modal frequency and mode shape data at the measured DOFs.

IV. Performance Metrics

Several metrics are used to evaluate the error of a predicted measure with respect to a reference measure. The first error metric proposed evaluates the relative quadratic point-to-point error at each DOF between the predicted expanded mode shape $\hat{\phi}_{Ni}$ and the actual measured mode shape $\tilde{\phi}_{Ni}$, for each mode i:

$$\Delta(i) = \frac{|\hat{\phi}_{Ni} - \tilde{\phi}_{Ni}|}{|\tilde{\phi}_{Ni}|} \tag{10}$$

In comparing mode shapes at each point, normalization of the eigenvectors is achieved by a least-squares fit of the expanded mode shape to the reference mode shape via

$$\hat{\phi}^{LS_{Ni}} = \rho\tilde{\phi}_{Ni}, \qquad \rho = \frac{\langle \tilde{\phi}_{Ni}, \hat{\phi}_{Ni}\rangle}{\langle \tilde{\phi}_{Ni}, \tilde{\phi}_{Ni}\rangle} \tag{11}$$

Alternatively, the mean cumulative error in the mode shape as a function of the nth mode can be used to determine the modal number at which the expansion methods start to break down:

$$C(n) = \frac{1}{n}\sum_{i=1}^{n}\Delta(i) \tag{12}$$

The orthogonality properties between two eigenvectors ϕ_i and ϕ_j, as inferred in the MAC, can also be used as performance metric, where

$$\mathrm{MAC}_{ij} = \frac{\left|\phi_i^T\phi_j\right|^2}{\left|\phi^{T_i}\phi_i\right|\left|\phi_j^T\phi_j\right|} \tag{13}$$

The MAC are used here to verify the orthogonality between the expanded mode shapes and the actual mode shapes measured at all DOFs. From Eq. (13) we see that the ideal MAC matrix is the identity matrix.

It is relatively straightforward to establish a relationship between the MAC and the normalized norm-squared difference between eigenvectors as in Eq. (10). To show this relationship, assume ϕ and ψ are two unit vectors. By orthogonal projection, we can write

$$\psi = \beta\phi + \epsilon$$

where β is a scalar and $\langle \epsilon, \phi \rangle = 0$. Now, note that $|\beta\phi + \epsilon|^2 = 1$ implies that for small ϵ,

$$\beta \approx 1 - (|\epsilon|^2/2)$$

Hence,

$$\mathrm{MAC}_{\phi\psi} \approx 1 - |\epsilon|^2 \tag{14}$$

On the other hand, we have

$$\begin{aligned} |\phi - \psi|^2 &= |(\beta - 1)\phi + |\epsilon|^2| \\ &= (\beta - 1)^2 + |\epsilon|^2 \\ &\approx |\epsilon|^2 \end{aligned}$$

Thus,

$$|\phi - \psi| \approx |\epsilon| \tag{15}$$

Comparing Eqs. (14) and (15), we see, for example, that a norm difference of 10% between two vectors is equivalent to MAC of approximately 0.99. Thus the norm error appears to be a significantly more sensitive measure of performance than the MAC.

A third performance metric uses global mass properties and is based on the MX of structural eigenvectors. The MX matrix between two eigenvectors ϕ_i and ϕ_j, is defined as

$$\mathrm{MX}_{ij} = \langle \phi_{Ni}, M\phi_{Nj}\rangle \tag{16}$$

In this study, MX is used to measure the mass cross-orthogonality of the expanded experimental mode shape with respect to the full experimental mode shape. If ϕ_i and ϕ_j are mass orthogonal, then MX is a diagonal matrix. Furthermore, if ϕ_i and ϕ_j are mass normalized, then MX is the identity matrix.

The three performance metrics discussed above are global metrics describing the total error throughout the whole set of DOFs. Errors also can be evaluated at the local structural element level by the strain energy distribution associated with each element s and with each mode i. Analogous to MX, which measures the accuracy of the expanded mode shape with respect to the FEM mass matrix M, the element modal strain energy verifies the fit of $\hat{\phi}_{Ni}$ with respect

to the FEM stiffness matrix K. In the following definition, $\hat{\theta}_{si}$ is the element modal strain energy, k_{ss} is the element stiffness, and $\hat{\phi}_{si}$ is the ith expanded mode shape at the element DOFs s; $\hat{\theta}_{si}$ is normalized with respect to the total strain energy for that mode:

$$\hat{\theta}_{si} = \frac{\langle \hat{\phi}_{si}, k_{ss}\hat{\phi}_{si} \rangle}{\langle \hat{\phi}_{Ni}, K\hat{\phi}_{Ni} \rangle} \tag{17}$$

The element strain energy error between the analytical θ_{Ni} and the expanded $\hat{\phi}_{si}$ identifies the discrete DOFs where the expansion does not agree with the model. Such errors typically result from localized modeling errors or actual structural damage.

V. Sensitivity Study of Expansion Methods

This section compares the expansion methods outlined in Sec. III with respect to the performance metrics defined in the preceding section. Several deviations from an ideal data set are considered. These include added noise in the measurements, use of different-size data sets and locations of measured DOF, inadequacy of the a priori model, and, finally, combinations of model form error and measurement error.

A. Expansion Method Performance with Respect to Nominal Data and Updated FEM Model

The expansion methods are first investigated for their reliability and intrinsic performance when all experimental and analytical conditions are ideal. The expansion is executed with the updated (i.e., ideal) FEM model and the measured mode shapes from a subset of the high-quality experimental data from the MPI test bed. The measured data are not corrupted by additional noise. Here, 12 locations have been retained as the measured set and are expanded to the full 240 DOFs recorded during the actual test. The final 240 DOF locations represent 3 DOFs at each of the 80 node balls forming the truss structure. The locations of the 12 DOFs are selected to give the best MAC with respect to the predicted analytical modes of the Guyan reduced model. This particular set of optimal instrument locations is referred to as aset 5. Other instrument locations are considered in Sec. V.C, which discusses the expansion sensitivity to DOF selection (Table 4). As will be demonstrated through the test cases, aset 5 provides enough information to identify the first nine modes, with the exception of mode 6, which is scarcely exhibited. The expansion of mode 6 thus will provide a measure of each method's robustness to poorly measured modal information.

The methods compared in this survey are Guyan, Eq. (1); Kidder, Eq. (2); Procrustes, Eq. (3); modal strain energy minimization with measurement error [PEN1, Eq. (5)]; modal strain energy minimization with Kidder expansion error [PEN2, Eq. (6)]; LSQI with measurement error [LSQI1, Eq. (7)]; LSQI with expansion error [LSQI2, Eq. (8)]; and LSQI with residual dynamic force minimization [LSQI3, Eq. (9)]. The MAC of the mode shapes expanded from experimental aset 5 data (12 DOFs) with respect to the actual full measurements (240 DOFs) is shown in Fig. 2 for all eight expansion methods. The MAC of the ideal analytical model with respect to the full 240 DOFs measurement set are also included in Fig. 2 for reference.

The Guyan method expands the first two modes properly with MAC greater than 0.98. However, modes 3–5 are poorly correlated, and modes 6–9 are not represented at all. PEN1 yields expanded mode shapes that have the same level of accuracy as the Guyan expansion. LSQI1 produces mode shape estimates that are slightly worse than the Guyan method, especially in the lower modes.

The Kidder method generates expanded mode shapes that have MAC greater than 0.97 for seven of the nine modes. Mode 9 has MAC of 0.90, and mode 6 could not be identified at all since it was not represented in the measurement set. Again, the PEN2 and LSQI2 yield the same level of accuracy as the Kidder expansion.

The Procrustes expansion method can predict mode 6, and produces MAC greater than 0.85 for all nine modes. However, only modes 1 and 3 are greater than 0.95. The mediocre results are explained by the fact that all nine modes are expanded simultaneously from the initial 12-DOF subset. In Sec. V.B, it is shown that the Procrustes method is very sensitive to the number of simultaneously expanded modes and to the set of measurement locations.

Table 4 Summary of instrument location cases

Aset no.	No. of instruments	Location criteria
1	3	1 per boom tip
2	6	best mode 1&2
3	6	2 per boom tips
4	12	triax @ boom tips
5	12	optimal MAC

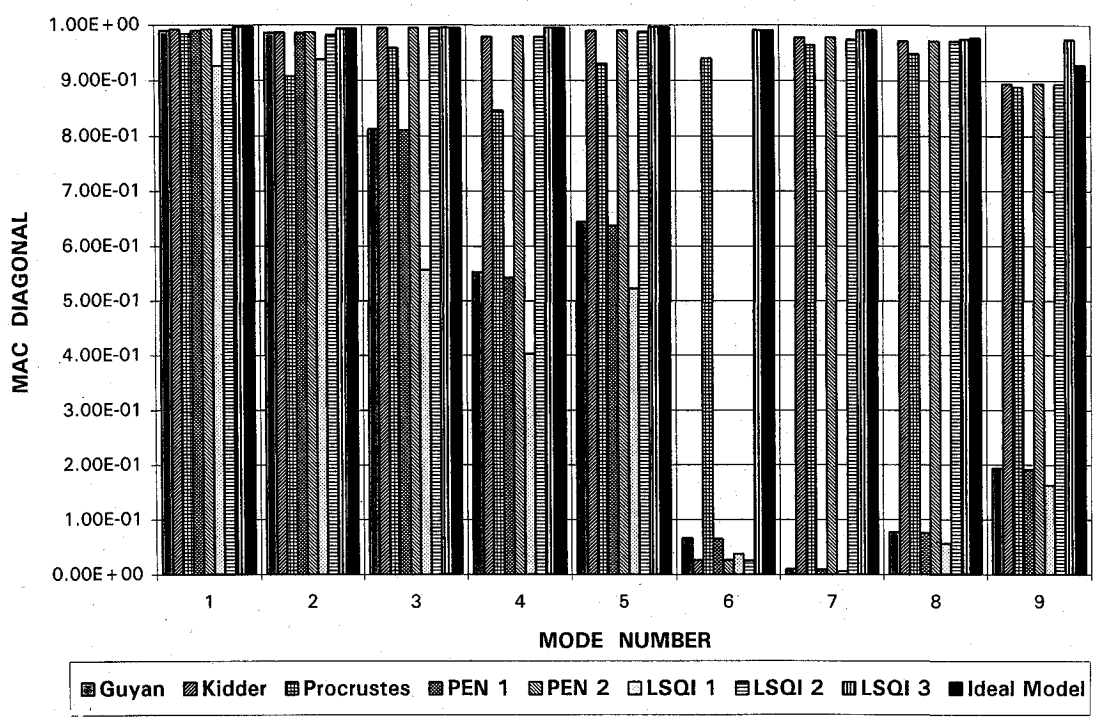

Fig. 2 Modal assurance criteria diagonals (measured vs expanded): expansion from aset 5 (12 DOFs) to 240 DOFs with ideal model and no additional measurement error.

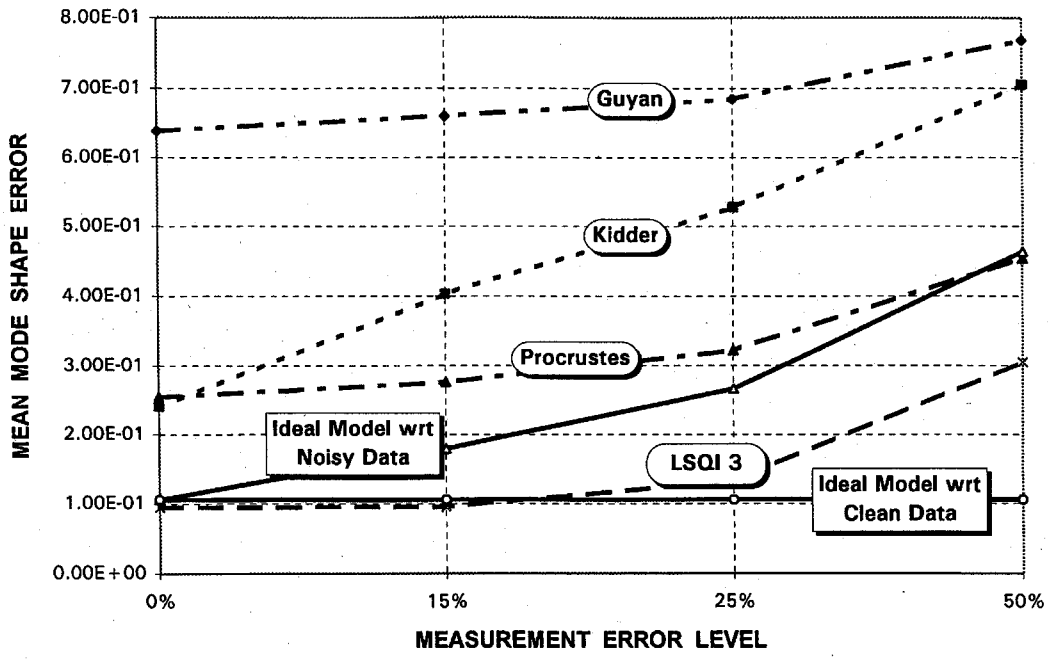

Fig. 3 Mean mode shape error as a function of measurement noise: expansion of nine modes from aset 5 (12 DOFs) to 240 DOFs with updated FEM model.

Of all the expansion methods, LSQI3 performs best across all modes. It is capable of predicting unmeasured mode 6 better than the Procrustes method. Foremost, it is the only expansion method that results in better MAC diagonals with respect to the measured data than the analytical model used to expand the modes.

The observations made on the performance of the expansion methods with respect to the MAC are consistent with the results obtained when considering the mode shape Frobenius norm error and the MX criteria [Eq. (16)].

B. Sensitivity to Mode Shape Measurement Errors

Noise in the measured-mode data can become important, especially when the expanded mode is used in strain energy computations for active member placement. Mode shape noise is still important, but to a lesser degree, when the extrapolated mode is used for computing elastic forces as is done in satisfying the modal force equilibrium equation to update FEM models. There are many sources of noise in the processing of mode shapes. Accelerometers, wires, and the method of data acquisition (e.g., number of averages). When transfer functions are processed to identify the mode shapes, an additional error can be introduced by the method of eigenvector computation (e.g., curvefitting or least squares). It suffices to say that the measured mode is never pristine. It is desirable, therefore, to have a mode shape extrapolation procedure that is not only insensitive to noise but that can filter it out as well.

A sensitivity analysis is performed herein to evaluate the performance of the mode shape extrapolation methods with respect to distributed measurement noise. For these investigations, the noise is represented as an additive Gaussian random error superimposed upon the true mode shape. Spatially localized errors are considered later in the context of isolated modeling errors and damage.

The Frobenius norm difference between the mode shapes obtained from the two independent tests were of the order of 15%. This level serves as a basis for the following error analysis. The performance of the expansion methods considers the effect of mode shape errors of the order of 15, 25, and 50%. Errors of the order of 50% are considered representative of gross experimental error, such as noisy or malfunctioning instrumentation, poor experimental procedures, or deficient modal estimation schemes. To infer the mean prediction, Monte Carlo simulations are performed with 30 averages. The analysis reveals that the penalty methods and the LSQI methods with strain energy minimization provide, at a very high computational cost, only a minor improvement in the predicted expansion compared with the Guyan or Kidder methods. The following performance evaluation thus is limited to the Guyan, Kidder, Procrustes, and LSQI3 methods.

The Frobenius norm error between the expanded and fully measured mode shapes is compared for the first nine modes of the MPI. The expansion is from aset 5 with 12 DOFs up to the full 240 DOFs, and is achieved with the updated ideal FEM model and eigenproperties. The results are summarized in Fig. 3, where the mean expansion error over the first nine mode shapes is plotted as a function of noise level for each of the expansion methods. The error between the ideal analytical mode shapes and the measured mode shapes at all DOFs with and without added measurement noise are included for comparison.

As expected, the performance of the expansion methods worsens as the noise in the measured data increases. As before, the Guyan method has the overall worst performance, followed by the Kidder and the Procrustes methods. The Kidder method is the most sensitive and exhibits linear growth in the mode shape error as a function of measurement error. The Guyan, Procrustes, and LSQI3 methods are equally sensitive to measurement noise, and a 15% noise level does not significantly increase the error in the expanded mode shape for any of these methods. Only when the noise level reaches 25% do differences appear. As in the ideal situation, the error in the modes expanded with the Guyan, Kidder, and Procrustes methods are greater than or equal to the error in the measurement. Only the LSQI3 method is capable of expanding mode shapes to a greater level of accuracy than the measured data, even when the original data are corrupted by significant amounts of noise. In fact, for moderate amounts of measurement noise (e.g., less than 25%) the first nine modes expanded with the LSQI3 method from 12 instrument locations to the full 240 DOFs are almost as accurate as the noise-free mode shapes measured at all DOFs. These remarks are consistent with the results from other performance metrics, such as the matrix norm error of the MAC or the MX for the first nine modes. These latter error norms are a measure of the projection of the set of expanded eigenvectors into the space of measured eigenvectors, and include both the diagonal and off-diagonal terms. Although the Procrustes method constructs the mode shape through an orthogonal projection, the LSQI3 method achieves better orthogonality with respect to the actual data set.

C. Sensitivity to Selection of Number of DOFs and Their Location

Five different sets of instrument locations and number of DOFs are considered, i.e., asets, as summarized in Table 4. The data measured at the aset location are expanded to the full 240 DOFs,

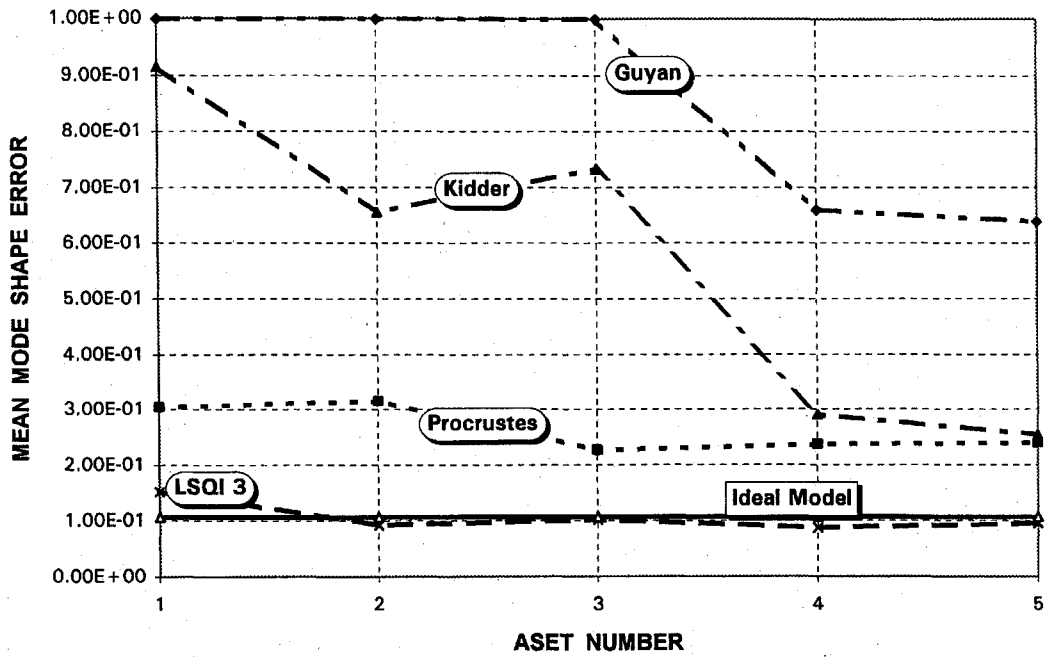

Fig. 4 Mean mode shape error as a function of instrument quantity and number (aset selection, Table 4): expansion of nine modes to 240 DOFs with updated FEM model and no additional measurement noise.

representing an expansion ratio of 1:80 for aset 1, 1:40 for aset 2 and aset 3, and 1:20 for asets 4 and 5. The instrument location is selected either according to engineering judgment at the DOFs of highest deformation (i.e., the tip of the boom, or according to optimality criteria such as best MAC fit from a static reduction or best mode shape fit over multiple modes).

The mean mode shape errors of the first nine modes [$C(n)$ from Eq. (12)] are summarized in Fig. 4 for each expansion method as a function of the aset selection. As expected, the expansion error decreases as the number of instrumented locations increases. Again, the Guyan method has the worst performance overall. Procrustes is the most sensitive to the aset selection, as shown by the 75% decrease in error from aset 1 to aset 5. The large errors for asets 1, 2, and 3 are to be expected, since the Procrustes method requires at least as many measured DOFs as modes to uniquely accomplish the orthogonal projection. Expansion with the Kidder method only benefits slightly by an increase in the number of DOFs. As before, only the LSQI3 method is capable of expanding the mode shape to the same degree of accuracy as the measured data, regardless of the selected aset. Figure 4 also shows the sensitivity of the expansion error to DOF location; asets 2 and 3 include the same number of DOFs but are located at different points on the structure. The performance of the Kidder method improved from aset 2 to aset 3, whereas the Procrustes method worsened. This implies that for optimal performance, each expansion method should have its own set of DOF selection criteria.

A separate analysis demonstrates that the Procrustes method is sensitive not only to the aset selection but also to the number of modes used in the simultaneous expansion and to the pairing between the analytical and experimental modes. This is a disadvantage compared with the Guyan, Kidder, and LSQI3 methods, which expand the modes individually without the need for mode pairing. In these latter methods, the mode pairing is indirectly accomplished through the FEM model and does not require any user input or engineering judgment. For the purpose of this analysis, the error in the expanded mode shapes is investigated for two alternative implementations of the Procrustes method. In the first method, modes 1–9 are expanded simultaneously using the first nine analytical modes, irrespective of the number of DOFs. In the second approach, the nth mode is expanded from the set formed by the first n analytical modes, disregarding the higher modes. This is referred to as the incremental form of the Procrustes method. Figure 5 shows the mean cumulative mode shape error for each of the methods from aset 3 (6 DOFs) to the full 240 DOFs, using the first nine modes. It is seen how, as expected, the simultaneous Procrustes has a poor performance, especially at the lower modes, because the number of expanded modes (9) exceeds the number of measured DOFs (6), whereas the incremental Procrustes has a good performance, similar to that of the Kidder and the LSQI methods up to mode 5. However, beyond mode 5, the performance of the incremental Procrustes deteriorates rapidly since the number of modes exceeds the number of measured DOFs. Thus, for this particular aset selection, the Procrustes method can only simultaneously expand the first five modes with accuracy from the 6 measured DOFs to the full 240 DOFs.

The same analysis is performed for the expansion from aset 5 (12 DOFs) to 240 DOFs, which includes twice as many measured locations as aset 3. The DOFs in aset 5 are located to provide the best orthogonality over the first nine modes, using a Guyan reduction in the analytical model. The main effect of aset 5 is to improve the accuracy of the Guyan and simultaneous Procrustes methods, especially in the lower modes for which the error is reduced by 80%. With aset 5, both Procrustes methods also converge toward a lower expansion error beyond the fifth mode. It is shown that the aset location criterion is a major factor in the reliability of the expansion method, and method-specific criteria must be devised to improve the performance.

D. Sensitivity to Model Error

All of the modal expansion methods proposed herein use the information derived from an analytical model to predict the mode shapes at the unmeasured DOFs. The FEM model plays an important role in the regularization of spurious information, the filtering out of the measurement error, and the prediction in the event of insufficient information. This is especially true of the Kidder and the LSQI3 methods, which rely heavily on the full dynamic equations. In the following, both distributed (i.e., global) and localized errors are investigated.

Distributed errors in the analytical mass or stiffness matrix, such as errors resulting from the uniform structural properties (e.g., mass density or modulus of elasticity), only scale the eigenvalue problem by a multiplicative constant. Thus, there is no change to the analytical eigenvectors, and, consequently, distributed property errors in the model have little influence on modal expansion prediction. Another form of global model error can be introduced by deficiencies in the model form, as would typically occur in a pretest model. For this effect, the actual pretest model of the MPI is used for demonstration. It is composed uniquely of rod elements that allow only axial deformations and can predict only the first four modes. The ideal updated

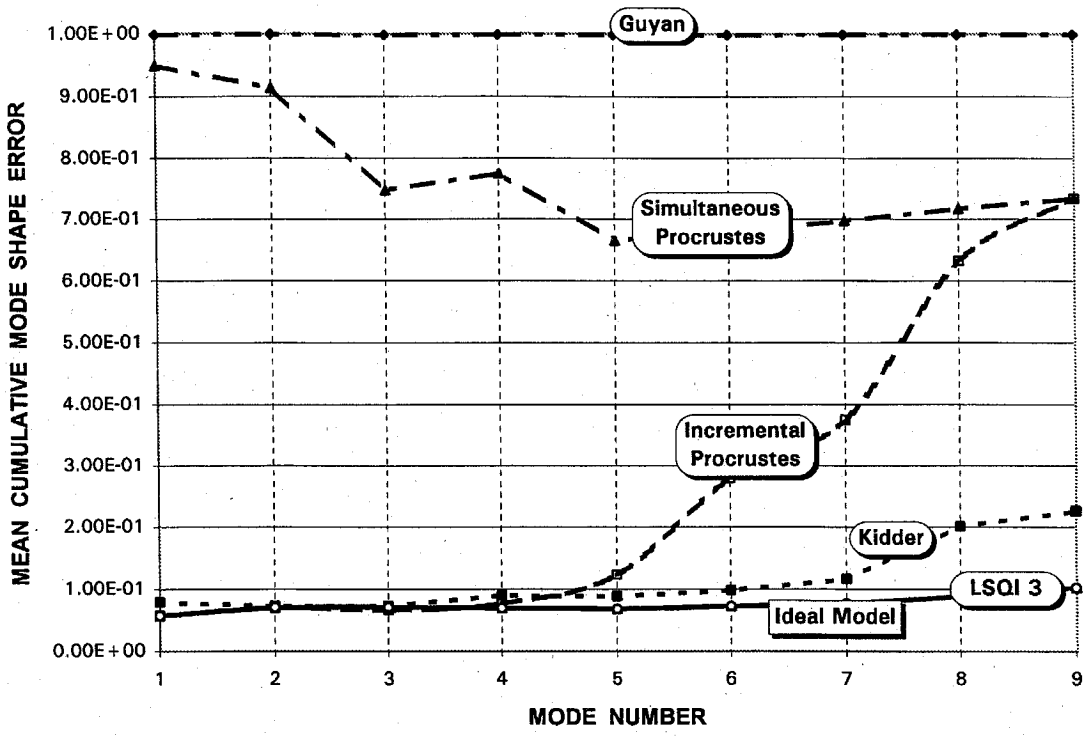

Fig. 5 Mean cumulative mode shape error: expansion from aset 3 (6 DOFs) to 240 DOFs with updated FEM model and no additional measurement noise.

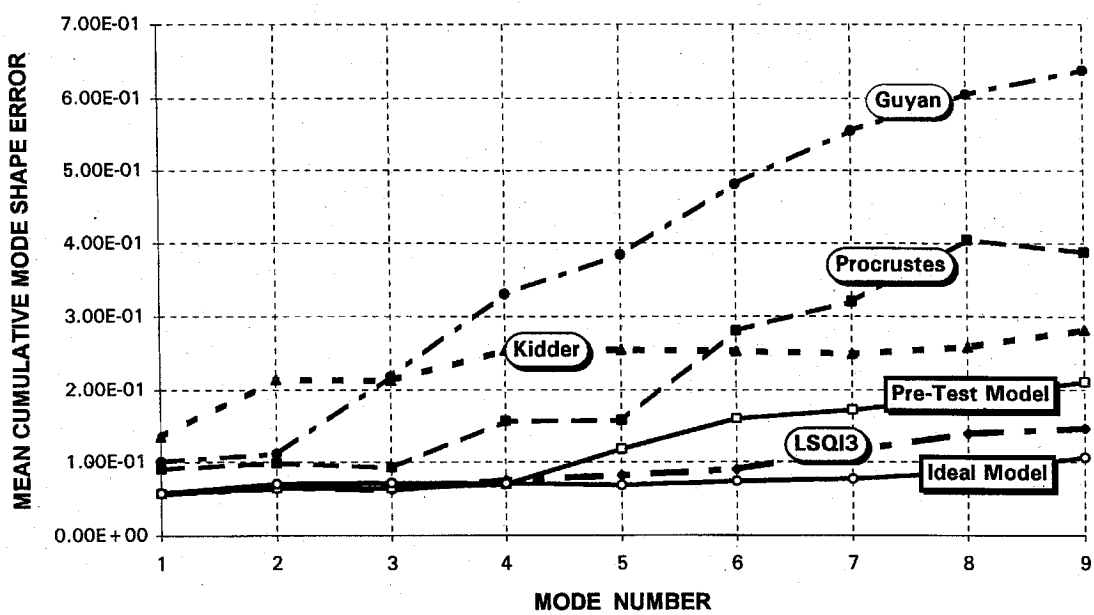

Fig. 6 Mean cumulative mode shape error: expansion from aset 5 (12 DOFs) to 240 DOFs with pretest FEM rod model and no additional measurement noise.

model is constructed uniquely of bar elements that allow both axial and bending deformations. This latter model can accurately predict the first nine modes. As shown in Fig. 6, the mean cumulative mode shape error over nine modes is 20% for the pretest rod model and only 10% for the updated bar model, which is below the expected experimental inaccuracies. The errors in the Guyan, the Kidder, the Procrustes, and the LSQI3 methods expanded with the pretest rod model from aset 5 to the full 240 DOFs are also shown in Fig. 6. As expected, the level of error is slightly worse when the eigenvectors are expanded with the pretest rod model than with the updated bar model, especially in the higher modes, where the accuracies of the pretest and updated model start to diverge. The Guyan and the Procrustes methods display little sensitivity to model form error. The Kidder method is the most sensitive, as is shown by the sharp increase in the error beyond mode 3, resulting in a mean error that is twice as high as that obtained with the updated model expansion. Although the performance of LSQI3 also has worsened, it is still the best by a factor of two relative to the other expansion methods, and it remains the only method that is capable of expanding mode shapes to a higher degree of accuracy than the model.

Spatially localized model error, such as would occur from local errors in the model form or properties, or from changes in the actual structure resulting from fatigue or damage, is also expected to affect the predictability of the expanded mode shapes. To simulate this situation, the stiffness of the longest strut in the pretest rod model, connecting the tower to the optics boom, is decreased by half. This only changes the pretest model frequencies of modes 5 and 6 by less than 3%, while keeping all other frequencies almost the same. However, the effect of this localized error on the analytical mode shapes is significant, as shown in Fig. 7, where a major jump in

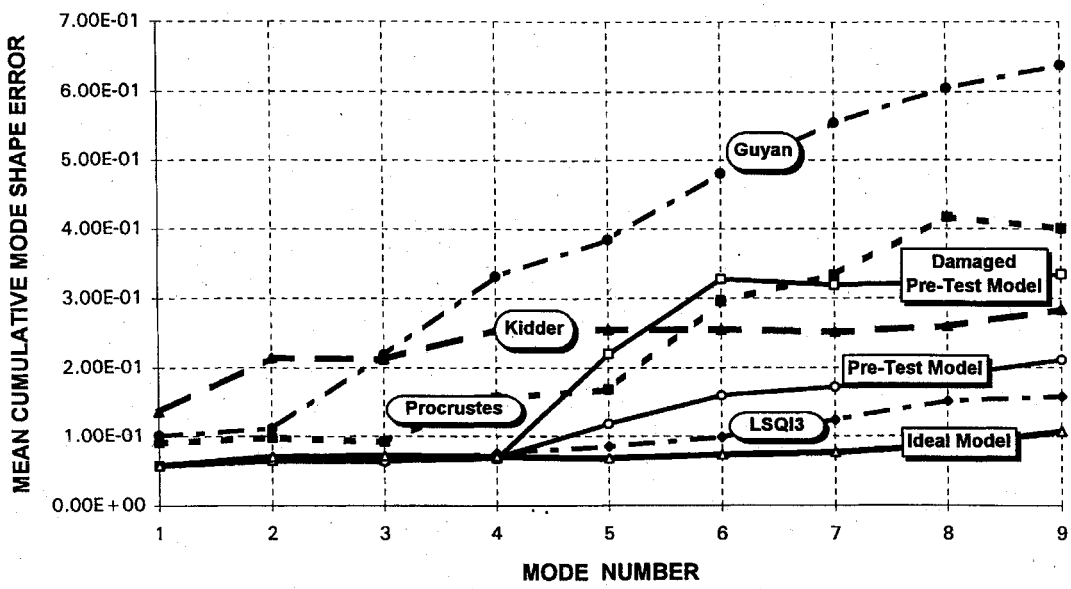

Fig. 7 Mean cumulative mode shape error: expansion from aset 5 (12 DOFs) to 240 DOFs with damaged pretest FEM rod model and no additional measurement noise.

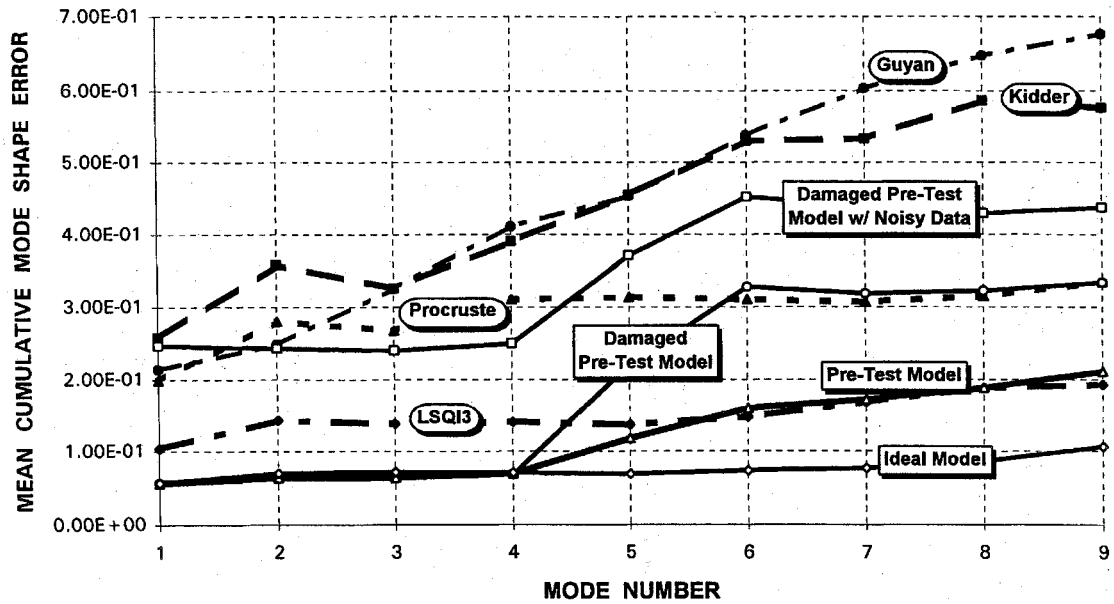

Fig. 8 Mean cumulative mode shape error: expansion from aset 5 (12 DOFs) to 240 DOFs with damaged pretest FEM rod model and 25% additional measurement noise.

modes 5 and 6 corresponds to a 300% increase in the mode shape error relative to the undamaged pretest model. All other mode shapes remain virtually unchanged. Although the effect on the analytical modes is extreme for modes 5 and 6, none of the expanded mode shapes is affected, and the expansion errors for each method are almost the same as those obtained previously with the undamaged pretest model (Fig. 6). The fact that the expansion error does not increase from the undamaged pretest model case implies that the expansion errors are more sensitive to global model form errors than to localized element errors.

The expanded mode shapes obtained here with the LSQI3 method are used to compute the element strain energy as defined in Eq. (17). When compared to the element strain energy predicted analytically by the damaged model, the largest differences occur in the damaged member. Thus, LSQI3 is capable of expanding mode shapes to the accuracy required to identify faulty elements in the model.

E. Sensitivity to Measurement and Model Error

Finally, to assess the performance of the expansion methods to a combination of modeling and measurement error, expansions were performed using the pretest model described above, which includes both model form error and localized model error, and using the actual experimental data with an additional 25% error in the measured mode shape values. The results are summarized in Fig. 8. The solid lines represent the accuracy of the different forms of the MPI model with respect to the true test data at all DOFs, and the dashed lines represent the expanded mode shapes from aset 5 to the full 240 DOFs using the damaged pretest model and noise-corrupted measurements.

As expected, using noisy data to expand the mode shapes from the damaged pretest model worsened the performance of all the expansion methods by approximately 50% (Figs. 7 and 8). In the presence of model error and measurement noise, the Guyan and Kidder methods perform equally poorly and generate mode shapes that are worse than predicted by the damaged pretest model. The Procrustes method performs better than the Guyan and the Kidder methods, especially at the higher modes; however, it cannot predict the modes to a better level of accuracy than the noise-contaminated data. Once again, the LSQI3 method performs exceptionally well. It generates mode shapes that are off by only 15%, although the data

used are contaminated by 25% noise and the model has the wrong form and a damaged member. Furthermore, comparison between the element strain energies of the damaged pretest model and LSQI3 expanded mode shapes show that the largest differences occur at the damaged-strut location. Thus, the mode shapes expanded with the LSQI3 method are capable of identifying damage or localizing model error, even in the presence of measurement noise.

VI. Further Results and Concluding Remarks

Several mode shape expansion methods have been proposed and investigated. These expansion techniques fall into three main categories. The first one uses direct solutions of the static and dynamic equations to obtain a closed-form equation. This category includes the Guyan and the Kidder methods. It is shown that these direct methods also can be written in terms of a constrained minimization problem. The second category uses a least-squares method to minimize the error between the measured and modeled eigenvectors. Within this category, the Procrustes method imposes orthogonality of the mode shapes. The third category formulates the expansion as a least-squares minimization problem with soft constraint. One approach incorporates the soft constraint as a penalty term; a second approach uses an inequality constraint. These constraints can depend on either the measured or an already expanded mode shape.

The trade study demonstrated that the LSQI method based on minimization of the dynamic force equation and subject to bounds imposed by measurement noise (LSQI3) has the best performance. The Procrustes method has a better performance than the direct methods but a worse performance than the LSQI3 method. The penalty methods and LSQI methods based on strain energy minimization yield results comparable to the Guyan or Kidder methods, even in the presence of large measurement noise and without any computational advantage.

The Guyan method can properly expand only the first few modes. To get a suitable expansion with the Guyan method, a good FEM model is necessary and a minimum ratio of 3 to 4 accelerometers per mode is required, as commonly practiced experimentally. Lower ratios of instrumented DOFs to modes and better performance can be achieved with the Procrustes, the Kidder, and the LSQI3. Under ideal experimental and analytical conditions, the Kidder method can correctly expand all modes represented in the data set. This method is not sensitive to the aset selection but is extremely sensitive to noise and model deficiencies. It was shown that the LSQI methods based on strain energy minimization did not improve on the accuracy of the direct methods, although they impose a significant computational cost. Computationally, the most efficient expansion method is the Procrustes method. Along with the LSQI3 method, it is the only method that can properly expand mode shapes that are not completely represented in the selected instrument locations. However, the Procrustes method can achieve this only if the analytical and experimental modes are properly paired. Pairing is automatically guaranteed in the other methods through the FEM model and the measured modal frequencies. Furthermore, the Procrustes method is very sensitive to measurement DOF location and selection, as well as to the number of simultaneously expanded modes. In an actual situation, this is a big disadvantage because the real solution is not known and the variation in the error can be great.

The LSQI3 expansion method with dynamic force minimization has the best overall performance. It is insensitive to moderate amounts of measurement error and is capable of predicting eigenvectors at unmeasured DOFs with greater accuracy than the noise-corrupted data measured at those locations. LSQI3 is the only method that is capable of regularizing global and local model errors, resulting in mode shapes of higher accuracy than the model originally predicted, even in the presence of experimental noise. New LSQI algorithms described in the companion paper[1] also make it more computationally efficient than with standard techniques.[8] This makes the LSQI expansion method with dynamic force minimization ideally suited for recursive model updating, damage detection, and response prediction technique.

Acknowledgment

The research decribed in this paper was carried out by the JPL, California Institute of Technology, under a contract with NASA.

References

[1]Levine-West, M., Milman, M., and Kissil, A., "Mode Shape Expansion Techniques for Prediction: Analysis," *AIAA Journal* (submitted for publication).

[2]Carne, T. G., Mayes, R. L., and Levine-West, M. B., "A Modal Test of a Space-Truss for Structural Parameter Identification," *Proceedings of the SEM 11th International Modal Analysis Conference* (Kissimmee, FL), Society for Experimental Mechanics, 1993, pp. 486–495.

[3]Red-Horse, J. R., Marek, E. L., and Levine-West, M. B., "System Identification of the JPL Micro-Precision Interferometer Truss: Test-Analysis Reconciliation," *Proceedings of the AIAA 34th Structures, Structural Dynamics, and Materials Conference* (La Jolla, CA), AIAA, Washington, DC, 1993, pp. 3353–3365 (AIAA Paper 93-1665).

[4]Neat, G. W., Sword, L. F., Hines, B. E., and Calvet, R. J., "Micro-Precision Interferometer Testbed: End-To-End System Integration of Control Structure Interaction Technologies," *Proceedings of the SPIE Symposium OE/Aerospace Science and Sensing, Conference on Spaceborne Interferometry* (Orlando, FL), 1993.

[5]Guyan, R. J., "Reduction of Stiffness and Mass Matrices," *AIAA Journal*, Vol. 3, No. 2, 1965, p. 380.

[6]Kidder, R. L., "Reduction of Structural Frequency Equations," *AIAA Journal*, Vol. 11, No. 6, 1973, p. 892.

[7]Smith, S. W., and Beattie, C. A., "Simultaneous Expansion and Orthogonalization of Measured Modes for Structure Identification," *Proceedings of the AIAA Dynamics Specialist Conference* (Long Beach, CA), AIAA, Washington, DC, 1990, pp. 261–270 (AIAA Paper 90-1218).

[8]Golub, G. H., and Van Loan, C. F., *Matrix Computations*, Johns Hopkins Univ. Press, Baltimore, MD, 1983.